Enhancing Electrochemical Reduction of CO_2 to Formate by Regulating the Support Morphology①

ZHAO Xiu-Hui[a, b] ZHUO De-Huang[a, b]
CHEN Qing-Song[b②] GUO Guo-Cong[②]
[a] (*College of Chemistry, Fuzhou University, Fuzhou* 350116, *China*)
[b] (*State Key Laboratory of Structural Chemistry, Fujian Institute of Research on the Structure of Matter, Chinese Academy of Sciences, Fuzhou* 350002, *China*)

ABSTRACT Electroreduction of CO_2 to formic acid has attracted extensive attention, because it is a promising strategy to re-utilize CO_2 and reduce greenhouse gas emissions that may favor the mitigation of energy and environment issues. Although great efforts have been made to tune the structure and composition of catalysts aiming to improve CO_2 conversion efficiency, seldom studies have been focused on the support regulation. In this work, ordered, porous TiO_2 nanotube arrays have been used as model support to study the impact of pore structure for CO_2 electrochemical reduction. It has been revealed that Pd supported on TiO_2 nanotube arrays substrate exhibits enhanced performance towards CO_2 reduction, showing a higher formate Faradaic efficiency of 20% over than Pd supported on TiO_2 film substrate. This study will shed new light on the design and synthesis of efficient catalysts by tuning the morphology of support for CO_2 conversion.

Keywords: CO_2ER, morphology, electrochemistry, formate; DOI: 10.14102/j.cnki.0254–5861.2011–2903

1 INTRODUCTION

With the rapid development of global industry, the economy has been significantly improved, and the demand for energy is dramatically increasing. The overexploitation and non-renewable characteristics of fossil energy may cause serious energy crisis. Meanwhile, a series of environmental problems appear because of the massive burning of fossil fuels and the excessive emission of CO_2, which is one of the main causes of greenhouse effect[1, 2]. Applying electrochemical method to convert CO_2 (CO_2ER) into valuable chemical fuels is a promising strategy to re-utilize CO_2 and reduce greenhouse gas emissions[3-5].

Among the various products of CO_2ER, formic acid (HCOOH) or formate is the most favorable. The way of CO_2ER to produce HCOOH is simple and only 2 electrons transfer in the whole electroreduction process. What's more, HCOOH is a liquid at normal temperature and pressure, which has various applications in many fields, such as a raw material for the industrial synthesis, a promising fuel candidate and a means of H_2 storage[6, 7]. However, due to the particular structure of CO_2, the characteristic of CO_2 is quite thermodynamically and kinetically stable[8], the energy barrier to CO_2ER is relatively high, converting CO_2 to HCOOH efficiently is not easy to achieve and it is required high overpotentials to initiate the process. A further significant issue is that under most reaction conditions, some side reactions such as hydrogen evolution will compete with CO_2ER, so that the result of Faradaic efficiencies of HCOOH product is getting lower[9]. Thus, the key point is to choose suitable electrocatalysts to improve the CO_2ER efficiency and reduce the required overpotentials.

It's reported that some metals can selectively convert CO_2 to HCOOH, such as Pd, Sn, Hg, Pb and Bi. Recently, some new electrocatalysts with high Faradaic efficiency (FE) have been researched in converting CO_2 to formate efficiently, such as Sn/*f*-Cu electrode[10], octahedron-shaped SnO_2 with exposed high-index {221} facets[11], HSA-Bi[12] and Bi_2S_3[7]. Nevertheless, CO_2 can be efficiently reduced to HCOOH at very low overpotential due to the unique structure of

Received 11 June 2020; accepted 9 July 2020
① This work was supported by the National Key R&D Program of China (2017YFA0206802, 2017YFA0700103), the Natural Science Foundation of China (21203200, 91545201) and the Natural Science Foundation of Fujian Province (2017J01036, 2018J06005)
① Corresponding authors. E-mail: chenqs@fjirsm.ac.cn and gcguo@fjirsm.ac.cn

PdH_xphase, and Pd-based catalysts are still considered to be the most promising cathode catalysts. As reported, the formation of a hydrogen-adsorbed Pd surface on a mixture of the α- and β-phases of a palladium-hydride core (α + β PdH_x@PdH_x) above −0.2 V(vs. RHE) facilitates HCOOH production via the HCOO* intermediate[13]. Kanan et al. dispersed Pd on a carbon carrier to synthesize a new catalyst. At a potential of −0.05 V (vs. RHE), the Faradaic efficiency of CO_2ER to HCOOH can be up to 100%, but when the potential was reduced to −0.35 V (vs. RHE), the corresponding value will be greatly reduced[14]. Rahaman et al. proved that the selectivity of CO_2ER is related to the particle size of Pd nanoparticles. They got Pd nanoparticles with different sizes by changing the concentration of PVP and temperature. Results showed that the selectivity of converting CO_2 to HCOOH reached as high as 98% at −0.1 V (RHE)[15]. Cai et al. demonstrated that the B doping in the Pd lattice interstices significantly impacts the pathways of CO_2ER and a Faradaic efficiency of ca. 70% for HCOOH has been obtained on Pd−B/C in a wide potential window[16].

Although the design and regulation of surface and electronic structures for the catalysts are important to improve their performance, there are still other factors which influence the activity of CO_2ER. For example, the structure and composition of the associated electrodes substrate were regarded as one of key points to maximize the activity of the catalysts on the electrodes[8, 9, 17, 18]. Since gas diffusion electrode (GDE) can promote the mass transport of CO_2 between the catalyst surface and the gas liquid interface by the special structure of three-dimensional network, it has been known as a candidate substrate for electroreduction of CO_2 to formic acid[17, 19, 20]. For example, tin electrodeposition on carbon fibers has been applied as GDE for CO_2ER[17]. Also, other designs for the structure of electrode substrates are available to improve the performance of CO_2 electrocatalysts. By synthesizing a series of ordered mesostructured Ag electrodes, researchers have proved that catalyst mesostructure improves the rate of the desired CO_2-to-fuels reaction as well as inhibiting the undesirable H_2 evolution reaction[18].

Herein, we used electrochemical anodization to synthesize an ordered TiO_2 nanotube arrays (TNTA) as a model porous electrode substrate. Comparing with TiO_2 nanofilm (TNF), TiO_2 nanotube arrays may enhance the catalytic performance for loaded Pd to catalyze CO_2 electrochemical reduction to formate. This study is of great importance to design electrocatalysts for CO_2 selective electroreduction to fuels by controlling the structure of electrode substrate.

2 EXPERIMENTAL

2. 1 Materials

All reagents were used without further purification. Ethylene glycol (AR), NH_4F (AR, 99%), $(NH_4)_2SO_4$ (AR, 99%), $PdCl_2$ (AR, 99%) and $NaBH_4$ (AR, 99%) were purchased from Sinopharm Chemical Reagent Co, Ltd. $KHCO_3$ (MACKLIN, 99.99%), D_2O (CIVI-CHEM, 99.9%) and Nafion (Alfa Aesar, 5wt%) were used as accepted. Nafion 117 membrane was purchased from DuPont (Wilmington, DE, USA) and Ti foil (0.1 mm thick, 99.0% purity) was used with pretreatment. CO_2 gas (99.9995%) was purchased from the YuanHua gas company. MilliQ ultrapure water (18.2 MΩ·cm) was used to prepare all aqueous solutions.

2. 2 Preparation of TiO_2 nanotube arrays (TNTA)

Firstly, Ti foil (0.1 mm thickness, 99.0% purity) was cut into pieces with a size of 1 × 2 cm^2. Then, they were cleaned by sonication in ethanol and acetone for about 30 min and washed with Millipore water (18 MΩ cm), and finally dried in air.

The electrolyte was ethylene glycol, containing 0.5 wt% of NH_4F and 6 vol.% Millipore water. TNTA was obtained by electrochemical anodization, which was carried out by a Maynuo DC Soure Meter and the voltage is 60 V for 0.5 h at room temperature[21-23]. Then the TNTA was heated to completely evaporate the solvent and annealed at 500 ℃ for 2 h in air.

2. 3 Preparation of TiO_2 nanofilm (TNF)

For the preparation of TNF, the pretreatment of Ti foil is similar. The preparation process of TNF was finished in an electrolyte containing 6.607 g $(NH_4)_2SO_4$ and 50 mL Millipore water. Platinum plate and the Ti foil were used as a counter electrode and working electrode, respectively. The anodization was carried out by a Maynuo DC Soure Meter at a voltage of 20 V for 1 min at room temperature. Then the solvent was evaporated and the TNF was annealed at 500 ℃ for 2 h in air.

2. 4 Preparation of Pd/TNTA and Pd/TNF

We used sequential chemical bath deposition[21] to load palladium nanoparticles on the electrode substrate. The as-synthesized substrate was firstly immerged in 0.03 M $PdCl_2$ solution for 30 s, then the substrate was washed in

Millipore water. Afterwards, the reduction of palladium was performed in 0.5 M $NaBH_4$ aqueous solution for 30 s. And then the sample was washed by pure water to remove the remaining reducing agent on the surface. The above procedures were repeated 6 times. Finally, the samples were dried in Ar atmosphere at room temperature.

2. 5 Physical characterizations

The morphology and the microstructure of electrodes were obtained from scanning electron microscopy (SEM, JSM6700F) operating at 15 kV and transmission electron microscopy (TEM, FEI Tecnai G2 F20) at 200 kV. An energy dispersive spectroscopy (EDS) microanalysis system was equipped on the microscope. Samples for TEM observations were prepared by scraping the Pd/TNTA and Pd/TNF from the substrate into 100 μL water and then drying a drop of dispersive suspensions on copper grids. The phase structures were examined by X-ray diffraction (XRD), which were obtained with a MiniFlex600 diffractometer (Rigaku) fitted with Cu$K\alpha$ (λ = 1.5406 Å) radiation in a reflection mode from 15^o to 80^o.

2. 6 Electrochemical measurements

All the electrochemical measurements of the electrodes were conducted with a Bio-Logic VMP3 potentiostat under ambient condition. The electrochemical experiment of electrodes was accomplished in 1 mol/L $KHCO_3$ aqueous solution in an H-type tight electrolytic cell, in which two compartments were separated by a Nafion 117 membrane. A saturated calomel electrode (SCE) was used as a reference electrode and a 1 cm^2 platinum plate as the counter electrode. The Pd/TNTA and Pd/TNF electrodes served as working electrodes. Before measurements, the CO_2 was bubbled into the electrolyte until it was saturated. And under the CO_2 electrolysis reaction, CO_2 was kept bubbling through the solution with a flow rate of 5 mL/min. When the electrolysis was finished, the Liquid products were analyzed by a 400 MHz NMR(Bruker AVANCE Ⅲ).

The Faradaic efficiency and partial current density of formate were calculated by the following equations:

$$\mathrm{FE}_{formate} = \frac{N \times F \times n_{\mathrm{HCOO^-}}}{Q_T} \times 100\% \quad (1)$$

$$j_{formate} = \frac{Q_T \times FE_{HCOO^-}}{t \times \mathrm{ECSA}} \quad (2)$$

where N is the number of electron transfers in the process of transferring CO_2 to formate (N = 2);

F is the Faraday constant (96500 C·mol^{-1});

$n_{\mathrm{HCOO^-}}$ is the amount of HCOOH which was calculated by the results of NMR; Q_T is the total charge integrated from the electrolysis curves.

The measurement and calculation of electrochemically active surface area (ECSA) is shown in supporting information.

3 RESULTS AND DISCUSSION

3. 1 Morphology characterizations

Fig. 1 shows the SEM images of the morphological features of TiO_2 nanotube arrays (TNTA) and TiO_2 nanofilm (TNF) as synthesized by electrochemical anodization. It is obvious that after the electrochemical etch assistant by NH_4F, the TNTA exhibits porous, highly ordered, compact and one dimensional features (Fig. 1a). The holes on it are arranged neatly and regularly. The average inner dimeter of the nano-tubes is about 70 nm and the thickness of nanotube wall is around 20 nm. Fig. 1b displays the morphology of TNF. Compared with TNTA, the difference is that the surface of prepared TNF is relatively smooth and has no rupture. The TNF sample shows much lower surface roughness than TNTA. It's reported that the porous structure in the materials can increase the density of grain boundaries and introduce more catalytically active sites[24]. Moreover, the porous structure of TNTA possesses higher surface area and enhanced mass transport that may serve as a better substrate than TNF.

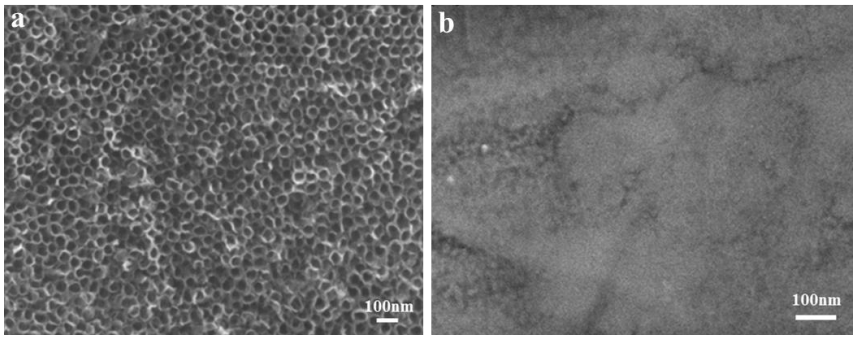

Fig. 1. SEM images of TNTA (a) and TNF (b)

The morphol ogies of Pd loading on TNTA and TNF (Pd/TNTA and Pd/TNF) by sequential chemical bath deposition were examined by SEM and TEM. The obvious Pd signal of Pd/TNTA appearing in EDS spectrum (Fig. S2) indicates that the palladium was loaded on the TNTA successfully. Meanwhile, the small peaks of Powder XRD which are attributed to metallic palladium phase can be observed in Fig. S3, offering another forceful evidence of Pd loading. From the SEM image of Pd/TNTA in Fig. 2a, the tube array structure keeps unchanged. After Pd loading on TNTA, many tiny particles and a few larger particles distribute well on the outer end of TNTA. The TEM image of Fig. 2b shows the cross-sectional view of as-prepared Pd/TNTA, which demonstrates that the Pd nanoparticles loaded not only on the top but also on the inner wall of the nanotubes. Moreover, the Pd nanoparticles with a small average diameter distribute well throughout the TiO_2 nanotubes without obvious agglomeration. In the case of Pd/TNF (Fig. 2c), the morphology of Pd/TNF is distinctly different to that of Pd/TNTA. EDS spectrum (Fig. S4) confirmed the palladium was also loaded on the TNF successfully. However, Pd nanoparticles with nonuniform size are aggregated dramatically to form a particle film on the surface of TNF substrate. The TEM image of Pd/TNF in Fig. 2d shows poor dispersity, and obviously, the larger Pd aggregates are assembled with amounts of tiny nanoparticles. In brief, the morphology of substrate impacts greatly on the structure of loading Pd nanoparticles, which may influence greatly on the performance of CO_2ER.

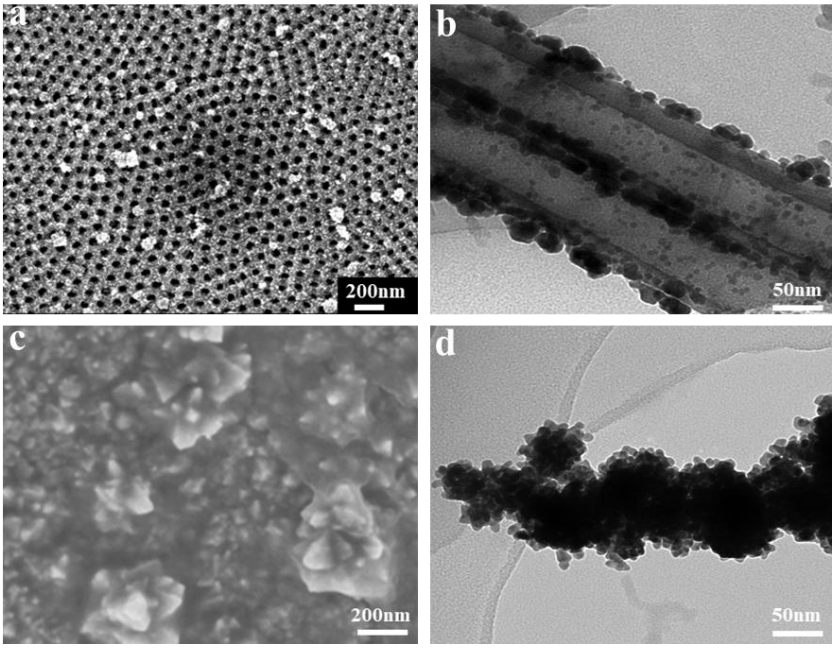

Fig. 2. SEM and TEM images of Pd/TNTA (a, b) and Pd/TNF (c, d)

3. 2 Electrocatalytic reduction of CO_2

In order to identify the electrocatalytic performance of Pd/TNTA and Pd/TNF electrodes, linear scan voltammetric characterizations were firstly carried out in CO_2-saturated 1 M $KHCO_3$ at a scan rate of 50 mV/s. Fig. 3 compares the LSV profiles of CO_2ER on Pd/TNTA and Pd/TNF electrodes. At low potential region, the current density of Pd/TNTA increases slowly with increasing the potential, while it increases much faster after the potential increases up to –0.68 V. This indicates that Pd/TNTA exhibits low overpotential towards CO_2 electrochemical reduction which is in good coincidence with previous reported Pd based catalysts[25, 26]. Moreover, in the whole potential region the current density of Pd/TNTA is always much larger than that of Pd/TNF, e.g., the current density of Pd/TNTA reaches a value of about –1.12 mA/cm^2 at –1.05 V while the corresponding value of Pd/TNF is only about –0.29 mA/cm^2, preliminary suggesting that the Pd/TNTA electrode is more active to convert CO_2.

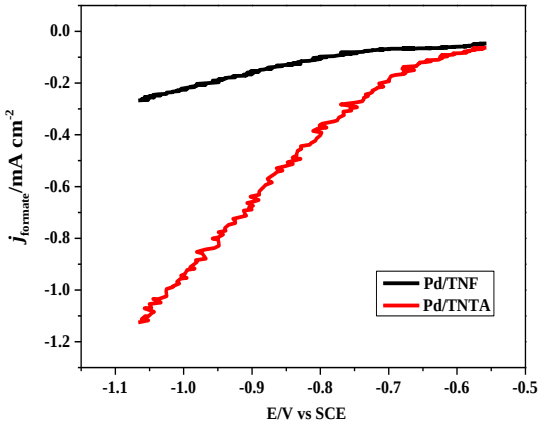

Fig. 3. Linear-sweep voltammograms (LSV) of Pd/TNTA and Pd/TNF in 1M CO_2-saturated $KHCO_3$ at a scanning rate of 50 mV/s

To better understand the influence of electrode substrate on the selectivity of CO_2 electrochemical reduction to formate, bulk electrolysis experiment was conducted in an H-type electrolytic cell in CO_2-saturated 1M $KHCO_3$ electrolyte for 1 h. The current time transient of CO_2ER on Pd/TNTA is shown in Fig. S5. It is clear that the current densities did not change too much during the electrolysis, indicating Pd/TNTA shows excellent stability for CO_2ER. As analyzed by NMR, the formate is the only liquid product. Fig. 4 shows the potential dependence of $FE_{formate}$ for CO_2ER on Pd/TNTA and Pd/TNF. We note that within the applied potential range, all $FE_{formate}$ of Pd/TNTA are higher than that of Pd/TNF. At –0.7 V, the $FE_{formate}$ of Pd/TNTA can be up to ~90% with a low overpotential. As the electrolysis potential decreases from –0.7 to –0.9 V, the Faradaic efficiency of formate decreased gradually, further decreasing the applied potential leading to a drastic decrease of $FE_{formate}$. This points out that the available potential window of Pd/TNTA for electrochemical reduction of CO_2 to formate is still rather limited. According to the study of Wang et al., the product of CO_2ER is greatly influenced by the hydrogen adsorbed state on Pd surface, i.e., the formation of the α+β PdH_x@PdH_x active phase above –0.2 V (vs RHE) facilitates the formate production[13]. The hydrogen adsorption and absorption on Pd depend strongly on the applied potential, i.e., a phase transition will occur from α+β PdH_x@PdH_x active phase to β PdH_x@Pd, and accordingly the main product of CO_2ER changes from formate to H_2 and finally to CO with the decrease of potential. The $FE_{formate}$ of CO_2 reduction on Pd/TNTA is ca. 20% higher than that of Pd/TNF. Our research results further point out that the activity and selectivity of CO_2 reduction to formate can not only be promoted by modification of substrate by B or N[27], but also can be improved by regulating the substrate structure with porous structure. The TNTA substrate with porous structure may favor the CO_2ER to formate through the following aspects, enhancing metal-support interaction that facilitates the high dispersive of loading Pd nanoparticles, enhancing adsorption capacity of CO_2[28], inhibition of the hydrogen evolution and improvement of the mass transport.

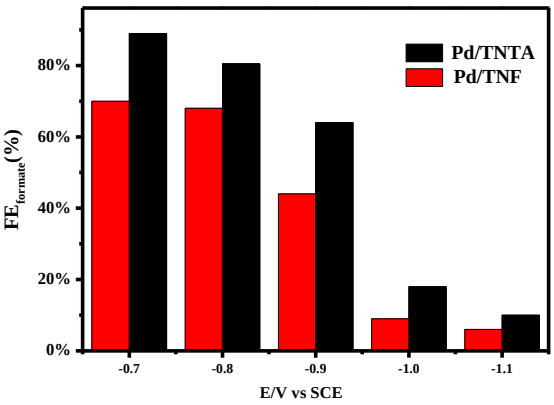

Fig. 4. $FE_{formate}$ of CO_2ER on Pd/TNF and Pd/TNTA at different applied potentials

4 CONCLUSION

In summary, we have successfully synthesized an ordered TiO_2 nanotube array (TNTA) as a model electrode substrate by electrochemical anodization. Pd nanoparticles were loaded on TNTA by a sequential chemical bath deposition. In comparison with Pd loading on TiO_2 film, the Pd nanoparticles loaded on TNTA showed higher dispersity with much lower size distribution. The ordered, porous TNTA supported Pd catalyst exhibits enhancing activity and selectivity for CO_2 electrochemical reduction to formate compared to the TiO_2 film supported Pd catalyst. The enhanced performance of Pd/TNTA can be attributed to the unique one-dimensional pore structure with large specific surface area that may enhance metal-support interaction and CO_2 adsorption, inhibit the hydrogen evolution and improve the mass transport. This study demonstrates that the design and regulation of the structures of catalyst supports are of significant importance for CO_2ER.

CONFLICTS OF INTEREST

There are no competing financial interests to declare.

REFERENCES

(1) Lu, Q.; Jiao, F. Electrochemical CO_2 reduction: electrocatalyst, reaction mechanism, and process engineering. *Nano Energy* **2016**, 29, 439–456.

(2) Zhu, D. D.; Liu, J. L.; Qiao, S. Z. Recent advances in inorganic heterogeneous electrocatalysts for reduction of carbon dioxide. *Adv Mater.* **2016**, 28, 3423–3452.

(3) Sarfraz, S.; Garcia-Esparza, A. T.; Jedidi, A.; Cavallo, L.; Takanabe, K. Cu–Sn bimetallic catalyst for selective aqueous electroreduction of CO_2 to CO. *ACS Catalysis* **2016**, 6, 2842–2851.

(4) Lu, Q.; Rosen, J.; Zhou, Y.; Hutchings, G. S.; Kimmel, Y. C.; Chen, J. G.; Jiao, F. A selective and efficient electrocatalyst for carbon dioxide reduction. *Nat Commun.* **2014**, 5, 3242.

(5) Aresta, M.; Dibenedetto, A.; Angelini, A. Catalysis for the valorization of exhaust carbon: from CO_2 to chemicals, materials, and fuels technological use of CO_2. *Chem. Rev.* **2014**, 114, 1709–1742.

(6) Zu, M. Y.; Zhang, L.; Wang, C. W.; Zheng, L. R.; Yang, H. G. Copper-modulated bismuth nanocrystals alter the formate formation pathway to achieve highly selective CO_2 electroreduction. *J. Mater. Chem. A* **2018**, 6, 16804–16809.

(7) Zhang, Y.; Li, F.; Zhang, X.; Williams, T.; Easton, C. D.; Bond, A. M.; Zhang, J. Electrochemical reduction of CO_2 on defect-rich Bi derived from Bi_2S_3 with enhanced formate selectivity. *J. Mater. Chem. A* **2018**, 6, 4714–4720.

(8) Avila-Bolivar, B.; Garcia-Cruz, L.; Montiel, V.; Solla-Gullon, J. Electrochemical reduction of CO_2 to formate on easily prepared carbon-supported Bi nanoparticles. *Molecules* **2019**, 24, 15.

(9) Zhou, F.; Li, H.; Fournier, M.; MacFarlane, D. R. Electrocatalytic CO_2 reduction to formate at low overpotentials on electrodeposited Pd films: stabilized performance by suppression of CO formation. *Chem. Sus. Chem.* **2017**, 10, 1509–1516.

(10) Wang, Y.; Zhou, J.; Lv, W. X.; Fang, H. L.; Wang, W. Electrochemical reduction of CO_2 to formate catalyzed by electroplated tin coating on copper foam. *Appl. Surf. Sc.* **2016**, 362, 394–398.

(11) Han, X. H.; Jin, M. S.; Xie, S. F.; Kuang, Q.; Jiang, Z. Y.; Jiang, Y. Q.; Xie, Z. X.; Zheng, L. S. Synthesis of tin dioxide octahedral nanoparticles with exposed high-energy {221} facets and enhanced gas-sensing properties. *Angew. Chem. Int. Ed. Engl.* **2009**, 48, 9180–9183.

(12) Zhang, H.; Ma, Y.; Quan, F. J.; Huang, J. J.; Jia, F. L.; Zhang, L. Selective electro-reduction of CO_2 to formate on nanostructured Bi from reduction of BiOCl nanosheets. *Electrochem. Commun.* **2014**, 46, 63–66.

(13) Gao, D.; Zhou, H.; Cai, F.; Wang, D. N.; Hu, Y. F.; Jiang, B.; Cai, W. B.; Chen, X.; Si, R.; Yang, F.; Miao, S.; Wang, J.; Wang, G.; Bao, X. Switchable CO_2 electroreduction via engineering active phases of Pd nanoparticles. *Nano Res.* **2017**, 10, 2181–2191.

(14) Min, X.; Kanan, M. W. Pd-catalyzed electrohydrogenation of carbon dioxide to formate: high mass activity at low overpotential and identification of the deactivation pathway. *J. Am. Chem. Soc.* **2015**, 137, 4701–4708.

(15) Rahaman, M.; Dutta, A.; Broekmann, P. Size-dependent activity of palladium nanoparticles: efficient conversion of CO_2 into formate at low overpotentials. *Chem. Sus. Chem.* **2017**, 10, 1733–1741.

(16) Jiang, B.; Zhang, X. G.; Jiang, K.; Wu, D. Y.; Cai, W. B. Boosting formate production in electrocatalytic CO_2 reduction over wide potential window on Pd surfaces. *J. Am. Chem. Soc.* **2018**, 140, 2880–2889.

(17) Irtem, E.; Andreu, T.; Parra, A.; Hernández-Alonso, M. D.; Garcá-Rodríguez, S.; Riesco-Garcá, J. M.; Penelas-Pérez, G.; Morante, J. R. Low-energy formate production from CO_2 electroreduction using electrodeposited tin on GDE. *J. Mater. Chem. A* **2016**, 4, 13582–13588.

(18) Youngmin, Y.; Anthony-Shoji, H.; Yogesh, S. Tuning of silver catalyst mesostructure promotes selective carbon dioxide conversion into fuels. *Angew. Chem. Int. Ed.* **2016**, 55, 15282–15286.

(19) Bitar, Z.; Fecant, A.; Trela-Baudot, E.; Chardon-Noblat, S.; Pasquier, D. Electrocatalytic reduction of carbon dioxide on indium coated gas diffusion electrodes — comparison with indium foil. *Appl. Catal. B-Environ.* **20**16, 189, 172–180.

(20) Machunda, R. L.; Ju, H.; Lee, J. Electrocatalytic reduction of CO_2 gas at Sn based gas diffusion electrode. *Curr. Appl. Phys.* **2011**, 11, 986–988.

(21) Chen, Y. X.; Lavacchi, A.; Chen, S. P.; Benedetto, F.; Bevilacqua, M.; Bianchini, C.; Fornasiero, P.; Innocenti, M.; Marelli, M.; Oberhauser, W.; Sun, S. G.; Vizza, F. Electrochemical milling and faceting: size reduction and catalytic activation of palladium nanoparticles. *Angew. Chem. Int. Ed. Engl.* **2012**, 51, 8500–8504.

(22) Jun, Y.; Park, J. H.; Kang, M. G. The preparation of highly ordered TiO_2 nanotube arrays by an anodization method and their applications. *Chem. Commun.* **2012**, 48, 6456–6471.

(23) Su, Z. X.; Zhou, W. Z. Formation, morphology control and applications of anodic TiO_2 nanotube arrays. *J. Mater. Chem.* **2011**, 21, 8955–8970.

(24) Kumar, B.; Atla, V.; Brian, J. P.; Kumari, S.; Nguyen, T. Q.; Sunkara, M.; Spurgeon, J. M. Reduced SnO_2 porous nanowires with a high density of grain boundaries as catalysts for efficient electrochemical CO_2-into-HCOOH conversion. *Angew. Chem. Int. Ed. Engl.* **2017**, 56, 3645–3649.

(25) Gao, D. F.; Zhou, H.; Cai, F.; Wang, J. G.; Wang, G. X.; Bao, X. H. Pd-containing nanostructures for electrochemical CO_2 reduction. *ACS Catal.* **2018**, 8, 1510–1519.

(26) Shao, X. Z.; Xu, J. M.; Huang, Y. Q.; Su, X.; Duan, H. M.; Wang, X. D.; Zhang, T. Pd@C_3N_4 nanocatalyst for highly efficient hydrogen storage system based on potassium bicarbonate/formate. *AIChE J.* **2016**, 62, 2410–2418.

(27) Bai, B.; Chen, Q. S.; Zhao, X. H.; Zhuo, D. H.; Xu, Z. N.; Wang, Z. Q.; Wu, M. Y.; Tan, H. Z.; Peng, S. Y.; Guo, G. C. Enhancing electroreduction of CO_2 to formate of Pd catalysts loaded on TiO_2 nanotubes arrays by N,B-support modification. *ChemistrySelect.* **2019**, 4, 8626–8633.

(28) Ma, S. C.; Lan, Y. C.; Perez, G. M. J.; Moniri, S.; Kenis, P. J. A. Silver supported on titania as an active catalyst for electrochemical carbon dioxide reduction. *Chemsuschem.* **2014**, 7, 866–874.